

# Design of MMIC Based on Mean Selection Method and Research the Model of MMIC Non-Dissipative MESFET

Bolin Ke, Chunhua Li, YANG Ai-Min  
Electronic Information Engineering College  
Zhejiang Wanli University  
No.8, South Qian Hu Road Ningbo, Zhejiang Province  
China  
<http://dxyy.zwu.edu.cn>

*Abstract:* Multi-object mean selection, an efficient method applicable to design mean of monolithic microwave integrated circuits (MMIC), is presented in this article. Based on theories of Monte Carlo analysis and yield histogram, this method first extracts multi-object mean points from yield histograms, then picks out optimal mean upon them by yield comparison. In the implementation of this method, a combination of interpolation sampling, parametric sampling and sample recognition methods is developed to improve Monte Carlo analysis, which keeps accuracy and attains more efficiency. With this advanced numeric physical models, the method of multi-object mean selection becomes far more accurate and reliable for MMIC designing. Analysis on the principle and characteristic of Non-dissipative MESFET mixer circuit has been discussed in detail in this paper. During research of CAD of this type of mixer, the technique of expanding the MESFET model has been offered. On the basis above, the 12.4~18GHz non-dissipative MESFET mixer have been designed. The mixer performs -3dB of conversion gain.

*Key-Words:* CAD; MESFET mixer; MMIC; Transfer characteristics; Local oscillation; Non-dissipative

## 1 Preface

MMIC is the microwave circuit made on semiconductor chip, with circuit functions communicated with traditional microwave circuit while quite different design methods. This is because all the components (including power parts and powerless components) of MMIC made on semiconductor chip must be plane structure. Though it's the same as traditional ones on name, it's different on performance. Complex models are needed to describe. On the other hand, the microwave transmission performance of semiconductor is quite different from traditional microwave chips, leading to the complex autoeciousness domino effect on microwave circuit with semiconductor chips as chip. It's a must to make professional design modifications. Moreover, MMIC chips always use microwave encapsulation while being used. So there's also specialty changes caused by the autoeciousness coupling of assembling and encapsulation themselves while chip are connected to encapsulation. The above-mentioned two reasons make the design of MMIC is generally much more complex than traditional microwave circuit. In addition, compared with traditional microwave circuit, the particularity of MMIC is more behaved on its unadjustability. MMIC is made by semiconductor integration

technology. Its specialty should be decided uniquely by design and production. It can't be the same as traditional microwave circuit in principle. Therefore, the design of MMIC must be reliable and realizable.

It is obvious that the design technology of MMIC has great particularity and complexity, having a pretty high demand on design optimization. Especially when thinking of the high manufacturing cost (thin line plate making, wafer craftwork and patch test etc.) of MMIC, we have to ask for a very high request on MMIC design engineers: the design must succeed once. Thus the workload of design optimization is far more than traditional microwave circuit and microwave integrated circuits. Meanwhile, as limited by craftwork control ability and precision in the course of making MMIC, different disperse exists in component specialty. Therefore, different from traditional microwave integrated circuits, the design of turnoff rate is needed in complete MMIC circuit design.

Aiming at the status of the rather bad craftwork level and low turnoff rate of MMIC, this article put forward mean design method which is a kind of circuit design CAD method facing the process of making integrated circuits. By simulating the random fluctuation of circuit geometry parameters, materials parameters and parameters in craftwork process in

the course of manufacturing, it estimates the end product rate that batch circuits can meet certain performance target and makes the end product rate reach the maximum by parameters mean optimization. The article optimizes through picking up multi target means selection and makes several improvements in allusion to the low efficiency that Monte Carlo analyzed in the process of design, greatly reducing circuits imitation quantity. The article calls this kind of calculation as multi-targets mean optimization.

Both satellite communication system and other microwave electronic system need high-performance mixer, while to reduce the useless power consumption plays a very important role in promoting the performance of the mixer. Monolithic microwave integrated circuit has become the major design direction of microwave electronic system. This paper puts forward one new design method for the design of the mixer of monolithic microwave integrated circuit. In recent years, the advantages of millimeter wavebands in the civilian and military fields are drawing popular attention from the people. We have applied or are considering applying this frequency spectrum to many new systems. In the emitting and receiving module of this kind of system, the most commonly-used millimeter wave part is mixer, its role to transform high-frequency signal into intermediate frequency signal, which is easy to be processed<sup>[1]</sup>.

In the useless power consumption of the MESFET mixer of monolithic microwave integrated circuit, the DC supply accounts for a large proportion, so it is very good choice to take off the MESFET drain DC supply. As shown in Fig 1, the circuit local oscillation (LO) of the mixer is input via MESFET drain and radio frequency (RF) signal is input via the grid while this mixer has no DC passage of MESFET drain. Driven by local oscillation power, MESFET enters nonlinear working region to realize the frequency conversion. Because MESFET is not supplied by drain DC and its static DC power consumption is zero, it is called no-DC-loss MESFET mixer, which makes it possible to reduce the DC power consumption of circuit. We have few documents, analyzing the working principles of this kind of mixer, and the common MESFET circuit module can't be directly used for adopting nonlinear analysis on this circuit, so this is why we need to study no-DC-loss MESFET mixer<sup>[2]</sup>.

## 2 Working Principles of No-DC-Loss MESFET Mixer

In the no-DC-loss MESFET mixer, as shown in Fig. 1,

MESFET is in nonlinear status. In working, MESFET will have  $V_{ds} < 0$  V and in analysis, we need to handle  $V_{ds} < 0$  of MESFET transfer characteristics. In analysis, we give the following assumptions:

(1) The transfer characteristic of MESFET adopts broken-line approximation and extends in  $V_{ds} < 0$  interval, as shown in Fig.2. The expression of drain-source circuit  $I_{ds}$  of MESEFT is as shown in (1). To reasonable simply this question, we only consider the first-order frequency conversion products of MESFET.

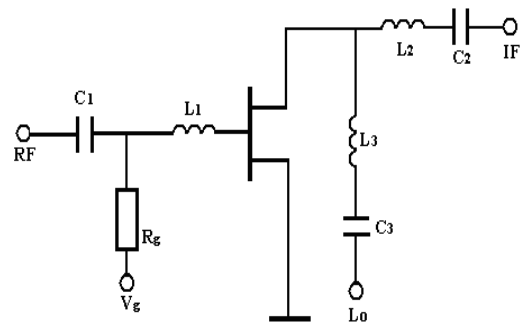


Fig.1 MESFET no-DC-loss mixer

(2) Between MESFET drain and sources displays short circuit for large signal of any frequency beyond direct circuit and local oscillation<sup>[3]</sup>.

As shown in the Fig,so:

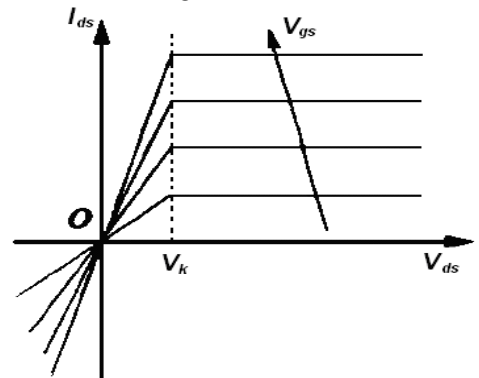


Fig.2 Broken-line approximation of MESFET transfer characteristics

$$I_{ds}(V_{gs}, V_{ds}) = \begin{cases} 0, & V_{gs} < V_{to} \\ \beta(V_{gs} - V_{to})^2, & V_{gs} \geq V_{to}, V_{ds} > V_k \\ \beta(V_{gs} - V_{to})^2 \frac{V_{ds}}{V_k}, & V_{gs} \geq V_{to}, V_{ds} \leq V_k \end{cases} \quad (1)$$

When grid and dra in apply fixed bias, we have

$$V_{gso} > V_{to}, \quad V_{ds} = V_{dso} + V_p \cos \omega_p t$$

$$I_{ds} = \begin{cases} \beta(V_{gs0} - V_{to})^2, & -\theta_m < \omega_p t < \theta_m \\ \beta \frac{(V_{gs0} - V_{to})^2}{V_k} (V_{dso} + V_p \cos \omega_p t), & \theta_m < \omega_p t < 2\pi - \theta_m \end{cases} \quad (2)$$

$$\theta_m = \arccos \frac{V_k - V_{dso}}{V_p} \quad (3)$$

Take Fourier transform on  $I_{ds}(t)$ , and let  $\omega_p t = \theta$ , then we obtain n-order components,

$$I_{dsn} = \frac{1}{2\pi} \left[ \int_{-\theta_m}^{\theta_m} \beta(V_{gs0} - V_{to})^2 e^{-jn\theta} d\theta + \int_{\theta_m}^{2\pi-\theta_m} \beta \frac{(V_{gs0} - V_{to})}{V_k} (V_{dso} + V_p \cos \theta) e^{-jn\theta} d\theta \right] \quad (4)$$

Among them, the DC component is:

$$I_{dso} = \frac{\beta(V_{gs0} - V_{to})^2}{\pi} \left[ \frac{V_{gs0}}{V_k} (\pi - \theta_m) - \frac{V_p}{V_k} \sin \theta_m + \theta_m \right] \quad (5)$$

Since the circuit and drain of non-DC-loss mixer don't apply DC working voltage, and using nonlinear characteristic that  $I_{ds}(t)$  of MESFET mixer has, the mixer can automatically establish DC operating point, and for the mixer circuit in Fig 1, the drain has no DC passage, we have  $I_{ds}(t) = 0$ , So

$$\frac{V_{dso}}{V_k} (\pi - \theta_m) - \frac{V_p}{V_k} \sin \theta_m + \theta_m = 0 \quad (6)$$

Solve the above equation, and we obtain self-constructed DC voltage  $V_{dso}$ . Fig3 shows  $V_{dso}$ 's change relationship with local oscillation voltage  $V_p$

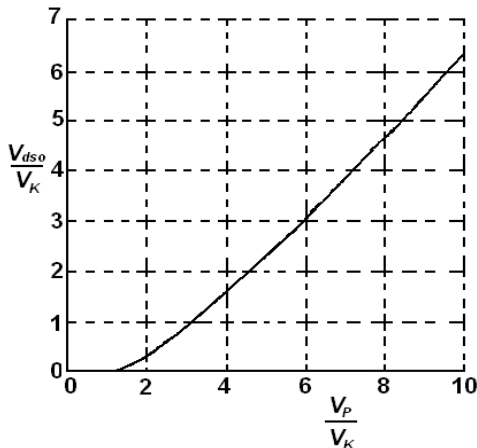


Fig.3 Research the model of MMIC Non-Dissipative MESFET

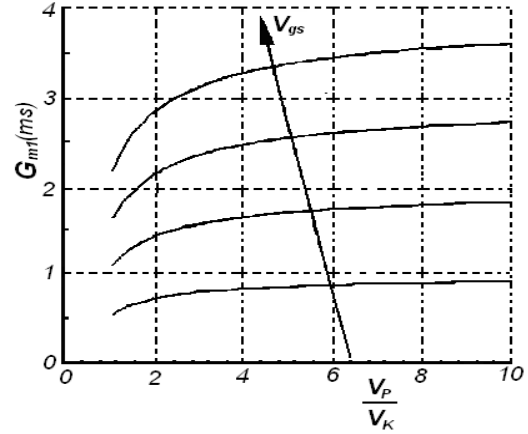


Fig.4 Change curve of conversion trans-conductance with  $V_p$

From the expression (2) of  $I_{ds}$ , we obtain nonlinear trans-conductance  $g_m$ :

$$g_m = \begin{cases} 2\beta(V_{gs0} - V_{to}), & -\theta_m < \omega_p t < \theta_m \\ 2\beta \frac{(V_{gs0} - V_{to})}{V_k} (V_{dso} + V_p \cos \omega_p t), & \theta_m < \omega_p t < 2\pi - \theta_m \end{cases} \quad (7)$$

Transform  $g_m$  into Fourier progression:

$$G_{mn} = \frac{1}{2\pi} \left[ \int_{-\theta_m}^{\theta_m} 2\beta(V_{gs0} - V_{to}) e^{-jn\theta} d\theta + \int_{\theta_m}^{2\pi-\theta_m} 2\beta \frac{(V_{gs0} - V_{to})}{V_k} (V_{dso} + V_p \cos \theta) e^{-jn\theta} d\theta \right] \quad (8)$$

Frequency conversion trans-conductance  $G_{m1}$  is:

$$G_{m1} = \frac{\beta(V_{gs0} - V_{to})}{\pi} \left[ (\pi - \theta_m) \frac{V_p}{V_k} + 2\left(1 - \frac{V_{dso}}{V_k}\right) \sin \theta_m - \frac{V_p}{2V_k} \sin 2\theta_m \right] \quad (9)$$

Change curve of frequency conversion trans-conductance with local oscillation driving voltage as shown in Fig4.

### 3 Study on Millimeter No-DC-loss MESFET module

#### 3.1 Extension Technique of MESFET Transfer Characteristic

The equivalent circuit module of MESFET generally is obtained via documents and direct measurement or manufactures and its empirical formulas all are obtained by the fitting under the condition of  $V_{ds} > 0$ , which are applicable for the application situation of  $V_{ds} > 0$ , but can not be directly applied to nonlinear circuit simulation under the condition of  $V_{ds} < 0$ .

According to the symmetry of physical structure of MESFET components, we directly extend module formula. After the extension, the value range of  $V_{ds}$  is allowed to be negative. Moreover, if keeping the symmetry of the original module, we can make the characteristic unchanged in the value range  $V_{ds} > 0$  of  $V_{ds}$ .

In MESFET module, the nonlinear channel current  $I_{ds}$  generally is expressed as the function between the gate-source and drain source voltage  $V_{gs}$  and  $V_{ds}$ , its format:

$$I_{ds} = I_{ds}(V_{gs}, V_{ds}), V_{ds} \geq 0 \quad (10a)$$

Applying Newton method to take iterative computation on harmonic balance equation, we also need to compute Jacobian matrix of the circuit, when we have to use  $I_{ds}$ , the derivative toward  $V_{gs}$  and  $V_{ds}$  (trans-conductance and self-conductance):

$$G_m = \frac{\partial I_{ds}}{\partial V_{gs}} = G_m(V_{gs}, V_{ds}) \quad (10b)$$

$$G_{ds} = \frac{\partial I_{ds}}{\partial V_{ds}} = G_{ds}(V_{gs}, V_{ds}) \quad (10c)$$

Because of the symmetry of physical structure of MESFET, as shown in Fig.5, the source and drain of MESFET can exchange operation, and even after the exchange the parameters of the module remain the same<sup>[4]</sup>, so

$$I'_{ds} = -I_{ds} \quad (11a) \quad V'_{ds} = -V_{ds} \quad (11b)$$

$$V'_{gs} = V_{gs} - V_{ds} \quad (11c)$$

Formula (10) is transformed into

$$\begin{aligned} I_{ds} &= -I'_{ds} = -I_{ds}(V'_{gs}, V'_{ds}) \\ &= -I_{ds}(V_{gs} - V_{ds}, -V_{ds}) \end{aligned} \quad (12a)$$

$$\begin{aligned} G_m &= \frac{\partial I_{ds}}{\partial V_{gs}} = -\frac{\partial I_{ds}(V'_{gs}, V'_{ds})}{\partial V_{gs}} \\ &= \frac{\partial I_{ds}(V'_{gs}, V'_{ds})}{\partial V'_{gs}} \frac{\partial V'_{gs}}{\partial V_{gs}} - \frac{\partial I_{ds}(V'_{gs}, V'_{ds})}{\partial V'_{ds}} \frac{\partial V'_{ds}}{\partial V_{gs}} \\ &= -G_m(V'_{gs}, V'_{ds}) = -G_m(V_{gs} - V_{ds}, -V_{ds}) \end{aligned} \quad (12b)$$

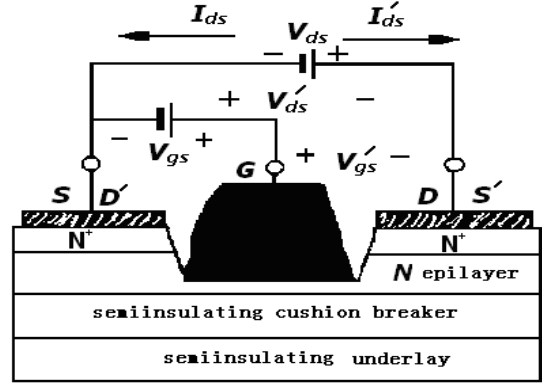


Fig. 5 Physical structure of MESFET, and voltage and current naming

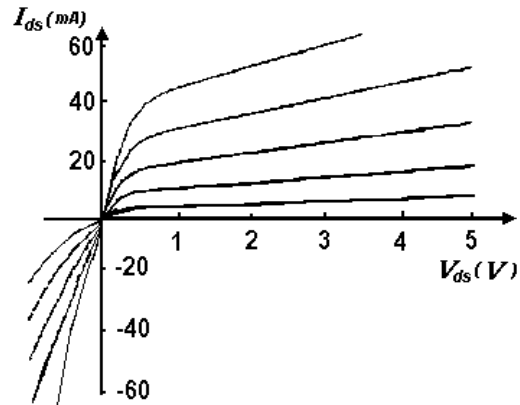


Fig.6 Extension of MESFET transfer characteristic curve.

$$\begin{aligned} G_{ds} &= \frac{\partial I_{ds}}{\partial V_{ds}} = -\frac{\partial I_{ds}(V'_{gs}, V'_{ds})}{\partial V_{ds}} \\ &= \frac{\partial I_{ds}(V'_{gs}, V'_{ds})}{\partial V'_{gs}} \frac{\partial V'_{gs}}{\partial V_{ds}} - \frac{\partial I_{ds}(V'_{gs}, V'_{ds})}{\partial V'_{ds}} \frac{\partial V'_{ds}}{\partial V_{ds}} \\ &= -G_m(V'_{gs}, V'_{ds})(-1) - G_{ds}(V'_{gs}, -V'_{ds})(-1) \\ &= G_{ds}(V_{gs} - V_{ds}, -V_{ds}) + G_m(V_{gs} - V_{ds}, -V_{ds}) \end{aligned} \quad (12c)$$

From the above, we obtain the transfer characteristic expression after the extension:

$$I_{ds} = \begin{cases} I_{ds}(V_{gs}, V_{ds}), & V_{ds} \geq 0 \\ -I_{ds}(V_{gs} - V_{ds}, -V_{ds}), & V_{ds} < 0 \end{cases} \quad (13a)$$

$$G_m = \begin{cases} G_m(V_{gs}, V_{ds}), & V_{ds} \geq 0 \\ -G_m(V_{gs} - V_{ds}, -V_{ds}), & V_{ds} < 0 \end{cases} \quad (13b)$$

$$G_{ds} = \begin{cases} G_{ds}(V_{gs}, V_{ds}), & V_{ds} \geq 0 \\ G_{ds}(V_{gs} - V_{ds}, -V_{ds}) \\ + G_m(V_{gs} - V_{ds}, -V_{ds}), & V_{ds} < 0 \end{cases} \quad (13c)$$

Fig.6 shows the precise extension curve of MESFET transfer characteristic. From the Fig, we know the broken-line approximation in the above principle analysis is right.

### 3.2 CAD Design of the Monolithic Circuit of the Mixer

The module parameters of MESFET play a decisive role in the performance of the mixer circuit. The current  $I_{ds}(V_{gs}, V_{ds})$  plays a frequency conversion role in the mixer circuit. The large-signal nonlinear characteristic of MESFET can be described in the following module formula:

$$I_{ds} = I_{dss} \left( \frac{V_{gs}}{V_p} - 1 \right)^2 \tanh \left( \frac{\alpha V_{ds}}{V_{gs} - V_p} \right) \quad (14)$$

among  $V_p = V_{po} + \gamma V_{ds}$  (15)

On the large-signal nonlinear characteristic of MESFET, we obtain the following module parameters:

$$\begin{aligned} I_{dss} &= 65mA \\ V_{po} &= -2.1V \\ \alpha &= 2.1V \\ \gamma &= -0.12 \end{aligned}$$

Fig.7 is the time domain waveform of MESFET in the cycle of local oscillation. Fig.8 shows the conversion gain of the MMIC mixer (local oscillation power 11dBm and 14dBm)

This method is applicable for the extension on the existing various component modules.

No-DC-loss MESFET mixer circuit has no DC power consumption and its circuit structure is simple, so it has better application prospect. The CAD design proposed in this paper of applying the extension technique of MESFET transfer characteristic to no-DC-loss MESFET mixer is successful.

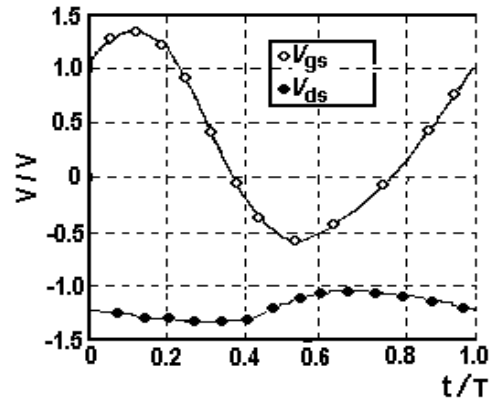


Fig.7 Time domain waveform of MESFET in the cycle of local oscillation

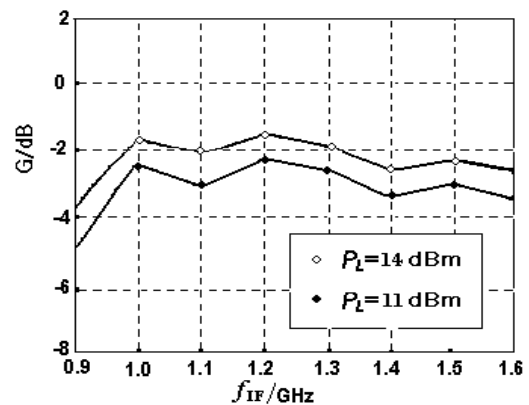


Fig.8 Computation result of conversion gain of Ku section mixer (local oscillation power)

## 4 Foundation of Mean Multi-Targets Optimization Concept

### 4.1 Estimation of Monte Carlo End Product Rate

Suppose the random fluctuation of MMIC parameters in the process of manufacturing meets united probability density function  $f(x, x_0)$ , all the circuit parameters are denoted by vectors as  $X = [x_1, x_2, x_3, \dots, x_M]^T$ . When defining circuit end product rate  $Y(x_0)$  as mean  $x_0$ ,  $x$  drops into the probability of  $R_a$ , hereinto,  $x_0$  is the mean of probability distribution. Suppose  $R_a$  is the eligible field formed by  $x$  that meets all the circuits' index. Get a eligible test function  $I(x)$ : if  $x \in R_a$  ( $x$  is eligible point),  $I(x)=1$ ; if  $x \notin R_a$  ( $x$  is disqualified point),  $I(x)=0$ . So,  $Y(x_0)$  can be denoted as the

mathematic expectation  $E\{I(x)\}$  of  $I(x)$ .

$$Y(x_0) = P(x \in R_a) = \int_{R_a} f(x, x_0) dx$$

$$= \int_{R^M} I(x) f(x, x_0) dx = E\{I(x)\}$$

As  $R_a$  is not, estimating  $E\{I(x)\}$  by adopting random average value, we get

$$Y(x_0) \approx \tilde{Y}(x_0) = \frac{1}{N} \sum_{n=1}^N I(x^n) \tag{16}$$

Formula (16) is the basic formula of Monte Carlo end product rate estimation. While estimating, according to probability density  $f(x, x_0)$ , N parameter random points  $x^n, n = 1, 2, \dots, N$  come into being, make circuit imitation for N times.

Calculating  $I(x^n)$ , we get  $\tilde{Y}(X_0)$  as the estimated value of  $Y(X_0)$ .  $\tilde{Y}(X_0)$  is non warp value of

$Y(X_0)$ . Estimated error is inverse ratio to N. Usually, we can get reliable convergent estimation result by 600-12000 times of circuit sampling imitation.

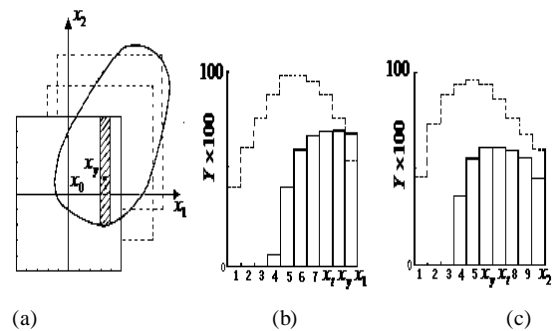
### 4. 2 Histogram of End Product Rate

End product rate histogram of circuit parameters is used to express the variation condition of end product rate while some circuit parameter  $x_m$  varies in its tolerance range. The horizontal axis divides the tolerance range of  $x_m$  into K sections equally. Take the median of each section  $x_{mk} k = 1, \dots, K$  as the datum mark of the section. The vertical axis shows the end product rate genes of each section pro rata, i.e., the end product rate  $Y(x_{mk})$  when  $x_m = x_{mk}$ . Figure 9 is a demonstration of end product rate histogram. In the figure, only two parameters  $x_1, x_2$ , equally distributed. Figure 9 (a) divides the tolerance area of each parameter into 10 sections. The oval circle is eligible field  $R_a$ . In Figure 9 (b), (c) shows the end product rate histogram of  $x_1, x_2$  separately. In the figure, real line means the histogram before optimization while broken line refers to the histogram after optimization.

Strict histogram of MMIC end product rate should make Monte Carlo analysis to each section of every circuit parameter, reasonably simplifying it.

Usually we substitute it with Monte Carlo analysis which has more once sampling points. Detailed methods are as below:

1) Equally divide the tolerance range of circuit parameter  $x_m, m = 1, \dots, M$  into K sections. Make Monte Carlo analysis with sampling time of N. Judge the value of  $I(x^n)$ , namely, whether  $x^n$  is eligible point or not.



(a) Section of circuit parameters  
(b) Histogram of  $x_1$   
(c) Histogram of  $x_2$

Fig.9 Demonstration of end product rate histogram

2) For each sampling point, judge which section each parameter fall into, and count the total sampling points  $N_{mk}$  and sampling eligible points  $N_{pmk}$  of each section.

3) Order  $Y_{mk} = \frac{N_{pmk}}{N_{mk}}$  as the end product rate of  $x_m$  section K, make end product rate histogram of all parameters.

### 4. 3 Target Mean Point

On real conditions, as factors of irregular eligible field and insufficient sampling, the histogram of end product rate is irregular with waving. Here, we specially consider the two characteristics on end product rate histogram:

1) Max tolerance point: the central point of the field formed by similar sections where end product rate is above certain fixed value  $Y_t$ , such as point  $x_t$  in Figure 9;

2) Max end product rate point: the central point of end product rate max section, such as point  $x_y$  in Figure 1. After picking up the above-mentioned characteristic point of each parameter, we get the mean  $x_y$  of max end product rate and the mean  $x_t$  of

max tolerance.  $x_y$  and  $x_t$  show the optimization direction of the two end product rates. Analysis results show, when the eligible field is narrow, the end product rate of  $x_y$  is usually better than that of  $x_t$ . While when the eligible field is wide, vice versa. Multi-target optimization choose  $x_y$ ,  $x_t$  and  $x_e$  as 3 basic target mean points. Through comparing end product rate, select the best value as one optimization result and repeat. The convergence speed of this optimization is quick. One time of repeat can greatly improve end product rate. Twice of three times of repeat can get very close to the best mean.

## 5 Betterment of Monte Carlo Analysis methods

### 5.1 Twice Inserted Value Sampling of Fixed Mode

By using inserted value sampling methods, we make some improvements on Monte Carlo analysis process as below: first, make imitation of few sampling points near mean, establish a normally suitable inserted value model and use inserted value model to make Monte Carlo analysis instead of circuit imitation. The precision and efficiency of inserted value sampling rest with the foundation of inserted value model. The inserted value model in this article takes the fixed mode twice inserted value model as basis. The quadratic polynomial approximately expresses the relation between circuit performance  $g(x)$  and circuit parameter  $x$  as below.

$$g(x) \approx q(x) = a_0 + \sum_{m=1}^M a_m (x_m - x_{jm}) + \sum_{\substack{m,l=1 \\ l \geq m}}^M a_{ml} (x_m - x_{jm})(x_l - x_{jl}) \quad (17)$$

Take reference point  $x_j$  as mean point. Pick up the following  $2M + 1$  fixed points to make sampling imitation. Make sure of all the modulus in formula (17)

$$\begin{cases} x^0 = x_j \\ x^m = x_j + [0, \dots, 0, \beta_m, 0, \dots, 0]^T, \\ x^{m+M} = x_j + [0, \dots, 0, \gamma_m, 0, \dots, 0]^T, \\ m = 1, 2, \dots, M \end{cases} \quad (18)$$

Here, we divide the tolerance field of  $x_{jm}$  into three parts by using average principle. The mean is in the center of the middle section. Take  $\beta_m, \gamma_m$  as the centers of the right and left section separately. Finally, taking  $2M + 1$  sampling points into the most plain quadratic modeling formula<sup>[9]</sup>, we can get all the modulus in formula (17).

The above-mentioned method can only make  $2M + 1$  times of imitations. Moreover, all modulus can resolve, taking out matrix calculation. However, all the quadratic cross items ( $a_{ml} = 0, m \neq l$ ) are ignored, bringing more errors to the circuits with strong parameter coupling efficiency while the function establishes models. The actual calculation shows, comparing with standard Monte Carlo method, errors of the end product rate gained through this method are usually within 10%.

### 5.2 Evaluation Methods of Parameters Sampling End Product Rate

Suppose we get the mean  $x_j$  after the  $j$  time of optimization whose end product rate  $Y(x_j)$  has been got in advance. For on point  $x'_j$ , its end product rate formula is:

$$Y(x'_j) \approx \frac{1}{N} \sum_{n=1}^N I(x^n) \frac{f(x^n, x'_j)}{f(x^n, x_j)} \quad (19)$$

$I(x^n)$  in the formula, meeting probability density  $f(x, x_0)$ , which was gained while estimating  $Y(x_j)$ . We can resolve  $Y(x'_j)$  by making use of the sampling imitation results while estimating  $Y(x_j)$ , no need to imitate again. In the selecting course of multi-target mean optimization, using parameter evaluation method can avoid making Monte Carlo end product rate estimation for every target point. As each target point is close to each other, we can get the end product rate of other target points by calculating on formula only through make Monte Carlo sampling imitation for one target mean point.

### 5.3 Inserted Value Sampling Updating Method Based on Sampling Identification

The fixed mode quadratic inserted value model is valid only in the neighbor field of mean, updating with the demand of repeating. If giving up the original model and imitating founding model again, the model precision can't be improved. This goes

against optimization convergence. If gradually changing model modulus through imitation as per the quadratic model updating arithmetic of Biernacki, we will lose the high efficiency of resolution. Therefore, this article keeps the modeling mode unchanged. We get the mean  $x_j$  after optimizing for J times, and found new model  $q_j(x)$  as per the methods in section 5.1. In the following Monte Carlo analysis, each time we take out one point  $x^n$ , we get all the model values  $q_j(x^n)$ ,  $j=0, 1, \dots, J$ , weighting average, expressed as  $g(x^n)$

$$g(x^n) = \frac{\sum_{j=0}^J w_j q_j(x^n)}{\sum_{j=0}^J w_j}$$

The confirmation methods of weighting modulus  $w_j$  ( $j = 0, 1, \dots, J$ ) is: for each model  $q_j(x)$ , find out the shortest distance  $L_j$  of the  $2M+1$  sampling points in  $x^n$  and formula(18); as in formula (18), on each sampling point,  $q_j(x) = g(x^n)$ , the less  $L_j$  is, the closer  $q_j(x^n)$  is to  $g(x^n)$ , so take  $w_j = L_j^{-p}$  ( $p$  is a whole number). This kind of confirmation methods adopts the concept of sampling identification. As the sampling points in formula (18) are very orderly, it's not needed at all to request distance point by point to confirm  $L_j$ . The whole updating method is high efficient.

## 6 Realization Approaches of Mean Optimization

1) Firstly found end product rate histogram, confirm 3 target mean points  $x_y, x_t$ , and  $x_c$ ;

2) Confirm optimization time J, initial mean  $x_0$  and their distribution  $f(x, x_0)$ , construct quadratic model  $q_0(x)$  as per the methods in section 5.1, calculate end product rate  $Y(x_0)$  through inserted value sampling, set  $x_{\max} = x_j, j = 0$ ;

3) For each point  $x_a$  in  $x_y, x_t, x_c$ , set  $x_a = x_j + h$ ; taking  $x_j$  as center, we get the condensation point  $x_{ac} = x_j + \alpha h, \alpha < 1$  and expansion point

$x_{ae} = x_j + \beta h, \beta > 1$  of  $x_a$  in the direction of  $h$ ; finally expand the target mean points to 9. Estimate the end product rate of the 9 target means at the same time by using formula (17), choosing the max end product rate point, endowed with  $x_{j+1}$ ;

4) Taking  $x_{j+1}$  as mean, construct quadratic model  $q_{j+1}(x)$ , calculate  $Y(x_{j+1})$  through inserted value sampling updating; if  $Y(x_{j+1}) \geq Y(x_j) - \Delta Y$  or  $j = J$ , finish optimization; or, set  $x_{\max} = x_{j+1}, j = j + 1$ , back to 1);

5) Best outputting mean  $x_{\max}$ .

To make sure of arithmetic convergence, increase the target mean points used for optimization by using the high efficiency of parameter sampling and set an error threshold  $\Delta Y$  to avoid comparing the end product rate wrongly. The above arithmetic adopts multi-target optimization concept, increasing the efficiency of MMIC design.

## 7 Examples of Mean Design

### 7.1 Example of MMIC Plain Plus Amplifier

This example designed the mean of a plain plus integrated amplifier. The design index is: frequency 10-14GHz, plus 8-10dB, circuit is like figure 10. All the length and width of guide strips in the figure are design parameters, 10 in total, meeting normal school. Tolerance is  $15\mu m$ . The transistor used is (MESFET) CFY18-23. Suppose all the parameters in it meet normal school, the tolerance is 1.5%.

By this method, we get the end product rate of initial mean is 72.3%, reaching 94.5% after the first optimization, 97.8% after second optimization and 100% after third optimization. Totally 78 times of circuit imitation.

### 7.2 Design example of MMIC High and Low Impedance Micro Strip Lowpass Design

Suppose index is  $f \leq 3GHz, \alpha \leq 1dB, f \geq 5GHz, \alpha \geq 20dB$ , circuit is like Figure 11. The 14 parameters in circuit all meet normal school, 10 sizes of which are design parameters,  $L_1 \sim L_5$  tolerance 6%;  $w_1, w_3, w_5$  tolerance 15%;  $w_1, w_4$  tolerance 10%. Tolerance of micro strip chip is 4%. Mean design

finishes after repeating for 5 times. Table 1 lists the end product rate  $Y_1$  after each optimizing and repeating and total amount  $N$  of circuit imitation. As comparison, we also show the standard Monte Carlo analysis results  $Y_2$  of 1000 times of sampling imitations.

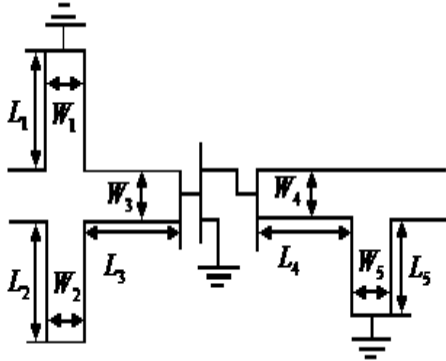


Fig.10 Demonstration of plain gain amplifier

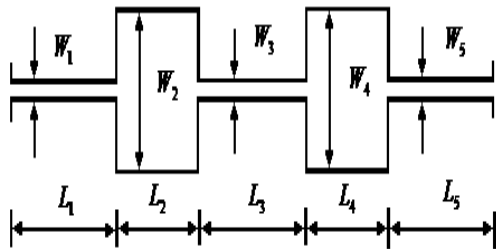


Fig.11 Demonstration of micro strip lowpass filter

**Table 1.** Mean optimization results of high and low impedance microstrip lowpass

	N	$Y_1 \times 100$	$Y_2 \times 100$
initial	27	40.6	44.0
first	54	75.7	75.3
second	81	86.4	84.2
third	108	87.2	88.1
fourth	135	90.1	90.6
fifth	162	93.1	92.9

Mean selection method put forward a kind of high efficiency multi-target optimization arithmetic aiming at the demand of MMIC mean design. Calculation examples show, this arithmetic can find out approximate best mean quickly and meanwhile get exact end product rate evaluation value, which means this method is effective and practical to MMIC design, making a foundation for introducing circuit numerical value model and realizing highly precise and reliable MMIC mean design.

*References:*

[1] Wang Ziqiang,Zhang Chun, Wang Zhihua,

Structure Design of Radio Receiver [J].Microwave Proceeds,2004,vol,34 NO.4:455~459.

[2] Zhang Shibing,Zhang Lijun Ultra-broadband Wireless Communication and Key Techniques [J]Telecommunication Techniques,2004,No.5,1-6.

[3] Stephen A.Maas,Fellow,IEEE,and Kwo Wei Chang A Broadband,Planar,Doubly Balanced Monolithic Ka-Band Diode Mixer, IEEE Trans on Microwave Theory and Technique.,vol41,No12,p2330~2335,Dec1993.

[4] DROR REGEV Characterization of Spurious Response Suppression in Double Balanced Mixer, IEEE Trans on Microwave Theory and Technique,vol 38,No2,pp123~128,Feb1990.

[5] Mac Farland A,Purviance P,Loescher D, et al.Centering and tolerancing the components of microwave amplifiers.IEEE MTT-S International Microwave Symposium Digest,1987.633~636.

[6] Cooke R,Purviance J.Statistical design for microwave systems.IEEE MTT -S International Microwave Symposium Digest,1991.679- 682.

[7] Singhal K,Pinel J.S statistical design centering and tolerancing using parametric sampling.IEEE Transaction on Circuits and Systems,1981,28: 692~701.

[8] Biernacki R,Bandler J,Song W,et al.Efficient quadratic approximation for statistical design. IEEE Transaction on Circuits and Systems,1989, 36 (11): 1449~1454.

[9] Biernacki R, Styblinski M. Statistical circuit design with a dynamic constraint approximation scheme.Proceedings of IEEE International Symposium on Circuits and Systems,1987.976~979.

[10] K.S.Yee.Numerical solution of initial boundary value problems involving Maxwell's equations in isotropic media[J].IEEE Tran.1966,AP-14, 302~307.

[11] D.M.Sheen et al.Application of the three dimensional finite difference time-domain method to the analysis of planar microstrip circuits [J].IEEE Trans.Microwave Theory Tech, 1990,38(7):849~ 857.

[12] R.Holland and J.W.Williams[J].IEEE Trans. Nucl.Sci.1983,(30):3483.

[13] Tong Li,Wenquan Sui.Extending PML Absorbing Boundary Condition to Truncate Microstrip Line in Nonuniform [J].IEEE Trans.On MTT, September 1999, 47 (9):724~ 730.

[14] Stephen D. Gedney. An Anisotropic Perfectly Matched Layer Absorbing Medium for the Truncation of FDTD Lattices [J ].IEEE Trans.on

- AP, December 1996, 44(12):1630~1639.
- [15] XiaoLei Zhang. Calculations of the Dispersive Characteristic of Microstrips by the Time-Domain Finite [J]. IEEE Trans. On MTT, 1988, 36:263~267.
  - [16] Clint Smith. LMDS: Local Multipoint Distribution Service [M]. McGraw Hill, 2000: 254.
  - [17] Singhal K, Pinel J. S. Statistical design centering and tolerancing using parametric sampling. IEEE Transaction on Circuits and Systems, 1981, 28: 692~701.
  - [18] Biernacki R, Bandler J, Song W, et al. Efficient quadratic approximation for statistical design. IEEE Transaction on Circuits and Systems, 1989, 36 (11): 1449~1454.
  - [19] Biernacki R, Styblinski M. Statistical circuit design with a dynamic constraint approximation scheme. Proceedings of IEEE International Symposium on Circuits and Systems, 1987. 976~979.
  - [20] Stephen A., Maas, Fellow, IEEE, and Kwo Wei Chang "A Broadband, Planar, Doubly Balanced Monolithic Ka-Band Diode Mixer," IEEE Transactions on Microwave Theory and Technique., vol 41, No 12, p2330~2335, Dec 1993.
  - [21] Mac Farland A, Purviance P, Loescher D, et al. Centering and tolerancing the components of microwave amplifiers. IEEE MTT-S International Microwave Symposium Digest, 1987. 633~636.
  - [22] Cooke R, Purviance J. Statistical design for microwave systems. IEEE MTT-S International Microwave Symposium Digest, 1991. 679~682.